Modulation of cation binding in calix[4]arene amides: synthesis, complexation and molecular modelling studies

Françoise Arnaud-Neu,[a] Silvia Barboso,[a] Frédéric Berny,[c] Alessandro Casnati,[b] Nicolas Muzet,[c] Alessandra Pinalli,[b] Rocco Ungaro,*[b] Marie-José Schwing-Weill*[a] and Georges Wipff*[c]

[a] *Laboratoire de Chimie Physique, UMR 7512 du CNRS, ULP-ECPM, 25, rue Becquerel, 67087 Strasbourg Cedex 2, France. E-mail: schwing@chimie.u.strasbg.fr*
[b] *Universita degli Studi di Parma, Dipartimento di Chimica Organica e Industriale, Area Parco delle Scienze 17/A, I-43100 Parma, Italy*
[c] *Laboratoire MSM, UMR 7551, Université Louis Pasteur, 4, rue Blaise Pascal, 67 000 Strasbourg, France*

Received (in Cambridge) 15th March 1999, Accepted 21st May 1999

We report combined experimental and theoretical studies on the complexation and liquid–liquid extraction of alkali and alkaline-earth cations by a series of calix[4]arenes bearing various combinations of primary, secondary and tertiary amide substituents. Four mixed calix[4]arene amides have been synthesized. Upon *N*-alkyl to *N*-H substitution on the amide binding sites, the binding strength of cations is reduced in methanol, and further, the extraction of cations from water into dichloromethane becomes highly inefficient. However, high complexation selectivities for Sr^{2+} and Ca^{2+} over Na^{+} are achieved for a mixed primary/tertiary derivative. The structures of typical free and complexed ligands are elucidated by NMR analysis and by molecular dynamics simulations in methanol and chloroform solution. Simulations at the water/organic interface also reveal different behaviour of tertiary/secondary/primary amide complexes.

Introduction

It is now well established that the nature of the substituents, both at the upper and lower rims, can play an important role in determining the efficiency and selectivity of cation extraction and complexation by calixarene ligands.[1] For instance, in calix[4]arene tetrafunctionalized podand type ligands it has been found that the metal ion complexation efficiency decreases in the series amide > keto > ester > ether, when these functional groups are used as chelating chains at the lower rim, and a much more complex picture emerges from ligands having a combination of functional groups.[1] The role of the substituents on the wide rim has recently been studied by some of us with calix[6]arene diethylamides: the change from *p-tert*-butyl groups to H induced spectacular changes in the binding affinities towards Na^{+} and Sr^{2+}cations, both in extraction and in complexation.[2] No similar studies were undertaken until now on the tetrameric amides, although it is known that *p-tert*-butyl calix[4]arene tetrakis(diethylamide) (**L1**) is a very powerful extractant and complexing agent of alkali and alkaline-earth cations.[3,4] In the case of amide binding groups there is also the opportunity to vary the type of the amide group (primary, secondary and tertiary) and explore its effect on the binding and extraction properties of the ligands. In fact, not only can the donor properties of the amide carbonyl group be varied by substitution at the nitrogen atom, but the presence of amide H atoms can also give rise to intra- or inter-molecular hydrogen bonding phenomena, which could affect the cation binding.[5] Most of the calixarene amides investigated are tertiary[3,6] and only in one case have qualitative extraction data on a calix[4]arene secondary amide ligand (**L2**) been reported.[7]

We present in this paper a systematic study of the synthesis, extraction, complexation and molecular modeling properties of primary, secondary and tertiary amide ligands (**L1**–**L6**), derived both from *p-tert*-butyl and *p*-H calix[4]arenes. Particular attention has been devoted to the Sr^{2+}/Na^{+} selectivity due to its importance in the treatment of radioactive waste.[8]

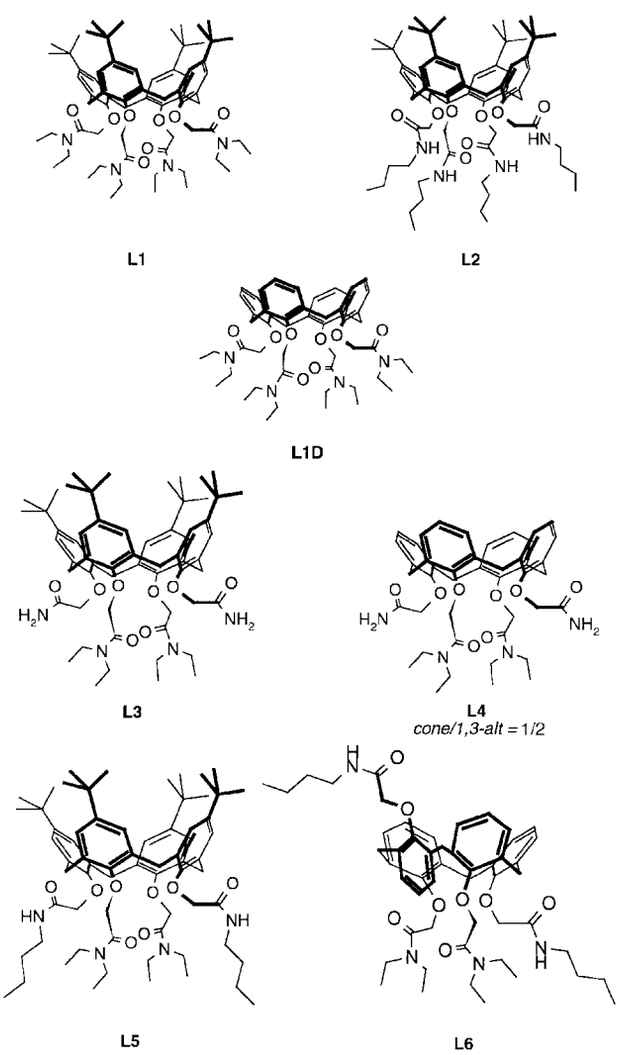

Experimental

Synthesis

Melting points were determined on an Electrothermal apparatus in sealed capillary tubes. Mass spectra (DCI, CH_4) were performed on a Finnigan MAT SSQ710 spectrometer. ^{1}H NMR and ^{13}C NMR spectra were recorded with Bruker AMX400 (^{1}H: 400 MHz) and AC300 (^{1}H: 300 MHz, ^{13}C: 75 MHz) spectrometers of the Centro Interdipartimentale di Misure (C.I.M.) of the University of Parma. Chemical shifts (δ) are expressed in ppm from $(CH_3)_4Si$; J values are in Hz. In NMR spectra, the Ar notation defines the aromatic nuclei of the calixarene backbone, considering the phenol oxygen as the main substituent to which the *ipso*, *ortho*, *meta* and *para* positions refer. IR spectra were performed on a Perkin-Elmer 298 spectrophotometer. All compounds gave satisfactory elemental analyses. All solvents were purified by standard procedures. Analytical TLC was performed on precoated silica gel plates (SiO_2, Merck, 60 F_{254}), while silica gel 60 (Merck, particle size 0.040–0.063 mm, 230–240 mesh) was used for preparative column chromatography. 25,26,27,28-Tetrakis(*N*,*N*-diethylaminocarbonylmethoxy)-*p*-*tert*-butylcalix[4]arene (**L1**),[3] tetrakis(*N*,*N*-diethylaminocarbonylmethoxy)calix[4]arene (**L1D**),[9] 25,27-bis(*N*,*N*-diethylaminocarbonylmethoxy)-*p*-*tert*-butylcalix[4]arene (**I**),[10] 25,27-bis(*N*,*N*-diethylaminocarbonylmethoxy)calix[4]arene (**II**),[10] and *N*-butyl-α-chloroacetamide[11] were prepared as described in the literature.

General procedure for the synthesis of mixed primary/tertiary amide calix[4]arene ligands (L3 and L4)

A sample of 25,27-bis(*N*,*N*-diethylaminocarbonylmethoxy)-calix[4]arene (**I** or **II**) (1.15 mmol) was dissolved in acetone (50 mL). To this stirred solution, K_2CO_3 (2.87 mmol), KI (2.87 mmol) and α-chloroacetamide (2.30 mmol) were added and the reaction mixture heated to reflux for 46 h (**L3**) or 12 h (**L4**). The solvent was removed under reduced pressure and the residue treated with 1 M HCl (75 mL) and CH_2Cl_2 (75 mL). The organic phase was separated, washed with water (75 mL), dried with $MgSO_4$, filtered and the solvent distilled off to give the crude product.

25,27-Bis(*N*,*N*-diethylaminocarbonylmethoxy)-26,28-bis(aminocarbonylmethoxy)-*p*-*tert*-butylcalix[4]arene (L3) (cone). By treating the crude product with hexane, pure compound **L3** was obtained as a white solid (yield 60%). Mp 252–254 °C; δ_H(300 MHz; $CDCl_3$; 300 K) 8.36 (2H, s, NH_2), 7.12 and 6.56 (8H, s, ArH), 6.10 (2H, s, NH_2), 4.81 (4H, s, OCH_2CO), 4.46 (4H, d, J 13.0, $ArCH_2Ar$, H_{ax}), 4.36 (4H, s, OCH_2CO), 3.43 (4H, q, J 7.0, $N(CH_2CH_3)_2$), 3.25 (4H, d, J 13.0, $ArCH_2Ar$, H_{eq}), 3.14 (4H, q, J 7.0, $N(CH_2CH_3)_2$), 1.33 (18H, s, $C(CH_3)_3$), 1.19–1.11 (6H, m, $N(CH_2CH_3)_2$), 0.85 (18H, s, $C(CH_3)_3$); δ_C(75 MHz; $CDCl_3$; 300 K) 173.1, 166.3 (s, CH_2CON), 150.7 (s, Ar *ipso*), 146.1, 146.0 (s, Ar *para*), 134.2, 131.4 (s, Ar *ortho*), 126.3, 125.2 (d, Ar *meta*), 73.9, 72.9 (t, OCH_2CO), 40.8, 40.2 (t, $N(CH_2CH_3)_2$), 33.7 (s, $C(CH_3)_3$), 31.5, 30.9 (q, $C(CH_3)_3$), 30.9 (t, $ArCH_2Ar$), 14.2, 13.0 (q, $N(CH_2CH_3)_2$); *m*/*z* 990 $(M + H)^+$ (Found: C, 72.72; H, 8.62; N, 5.80. $C_{60}H_{84}O_8N_4$ requires C, 72.85; H, 8.55; N, 5.66%).

25,27-Bis(*N*,*N*-diethylaminocarbonylmethoxy)-26,28-bis(aminocarbonylmethoxy)calix[4]arene (L4) cone : 1,3-alternate = 1 : 2. Pure compound **L4** was obtained by column chromatography (SiO_2: $CHCl_3$–acetone = 7 : 3) of the crude product followed by precipitation with hexane. Compound **(L4)** was obtained as a mixture of cone and 1,3-alternate conformations (1 : 2) in 72% yield. Mp of the mixture: 151–152 °C; *m*/*z* 765 $(M + H)^+$ (Found: C, 68.98; H, 6.96; N, 7.45. $C_{44}H_{52}O_8N_4$ requires C, 69.09; H, 6.85; N, 7.32%). Cone: δ_H(300 MHz; $CDCl_3$; 300 K) 8.43 (2H, t, NH_2), 7.10 (4H, d, J 7, ArH *meta*), 6.82 (2H, t, J 7, ArH *para*), 6.50 (4H, d, J 6, ArH *meta*), 6.40 (2H, t, J 6, ArH *para*), 6.18 (2H, s, NH_2), 4.67 (4H, s, OCH_2CO), 4.56 (4H, d, J 13.8, $ArCH_2Ar$, H_{ax}), 4.53 (4H, s, OCH_2CO), 3.40 (4H, q, J 7.1, $N(CH_2CH_3)_2$), 3.27 (4H, d, J 13.8, $ArCH_2Ar$, H_{eq}), 3.11 (4H, q, J 7.1, $N(CH_2CH_3)_2$), 1.17–1.08 (12H, m, $N(CH_2CH_3)_2$); δ_C(75 MHz; $CDCl_3$; 300 K) 170.4, 166.5 (s, CH_2CON), 154.9, 154.2 (s, Ar *ipso*), 134.3, 133.1 (s, Ar *ortho*), 131.4, 129.7 (d, Ar *meta*), 123.6, 122.9 (d, Ar *para*), 73.9, 71.9 (t, OCH_2CO), 41.5, 40.3 (t, $N(CH_2CH_3)_2$), 30.3 (t, $ArCH_2Ar$), 12.8 (q, $N(CH_2CH_3)_2$). 1,3-Alternate: δ_H(300 MHz; $CDCl_3$; 300 K) 7.07 (4H, d, J 7, ArH *meta*), 6.85–6.78 (8H, m, ArH), 6.72 (2H, s, NH_2), 5.34 (2H, s, NH_2), 4.21 and 4.07 (4H, s, OCH_2CO), 3.97 (4H, d, J 15.6, $ArCH_2Ar$), 3.70 (4H, d, J 15.6, $ArCH_2Ar$), 3.39 and 2.96 (4H, q, J 7.0, $N(CH_2CH_3)_2$), 1.20 and 0.87 (6H, t, J 7.0, $N(CH_2CH_3)_2$); δ_C(75 MHz; $CDCl_3$; 300 K) 170.8, 166.3 (s, CH_2CON), 154.2, 153.4 (s, Ar *ipso*), 135.5, 132.8 (s, Ar *ortho*), 129.3, 129.2 (d, Ar *meta*), 124.4, 123.5 (d, Ar *para*), 72.5, 68.1 (t, OCH_2CO), 40.6, 40.1 (t, $N(CH_2CH_3)_2$), 36.8 (t, $ArCH_2Ar$), 14.3 (q, $N(CH_2CH_3)_2$).

General procedure for the synthesis of mixed secondary/tertiary amide calix[4]arene ligands (L5 and L6)

A sample of 25,27-bis(*N*,*N*-diethylaminocarbonylmethoxy)-calix[4]arene (**I** or **II**) (1.5 mmol) was dissolved in acetonitrile (50 mL). To this stirred solution, K_2CO_3 (4.5 mmol), KI (4.5 mmol) and α-chloro-*N*-butylacetamide (4.5 mmol) were added and the reaction mixture heated to reflux for 54 h (**L5**) or 12 h (**L6**). The solvent was removed under reduced pressure and the residue treated with 1 M HCl (75 mL) and CH_2Cl_2 (75 mL). The organic phase was separated, washed with water (75 mL), dried with $MgSO_4$, filtered and the solvent distilled off.

25,27-Bis(*N*,*N*-diethylaminocarbonylmethoxy)-26,28-bis(*N*-butylaminocarbonylmethoxy)-*p*-*tert*-butylcalix[4]arene (L5) (cone). Pure compound **L5** was obtained by column chromatography (SiO_2: hexane–ethyl acetate = 1 : 9): (yield 52%). Mp 291–293 °C; δ_H(300 MHz; $CDCl_3$; 300 K) 8.01 (2H, t, J 6, N*H*R), 7.14 and 6.96 (4H, s, ArH), 4.60 and 4.57 (4H, s, OCH_2CO), 4.38 (4H, d, J 12.4, $ArCH_2Ar$, H_{ax}), 3.54 (4H, q, J 6.8, $N(CH_2CH_3)_2$), 3.33 (4H, d, J 12.4, $ArCH_2Ar$, H_{eq}), 3.28–3.19 (8H, m, $N(CH_2CH_3)_2$, $NHCH_2(CH_2)_2CH_3$), 1.61–1.51 (8H, m, $NHCH_2(CH_2)_2CH_3$), 1.30 and 1.22 (6H, t, J 6.8, $N(CH_2CH_3)_2$), 1.19 and 1.05 (18H, s, $C(CH_3)_3$), 0.92 (6H, t, J 7.2, $NH(CH_2)_3CH_3$); δ_C(75 MHz; $CDCl_3$; 300 K) 168.7, 167.9 (s, CH_2CON), 150.1, 149.9 (s, Ar *ipso*), 147.9, 147.1 (s, Ar *para*), 134.6, 133.5 (d, Ar *ortho*), 125.7 (s, Ar *meta*), 76.1, 73.5 (t, OCH_2CO), 40.9, 40.7 (t, $N(CH_2CH_3)_2$), 38.9 (t, $NHCH_2R$), 34.0, 33.8 (s, $C(CH_3)_3$), 31.4 (t, $ArCH_2Ar$), 31.2, 31.0 (q, $N(CH_2CH_3)_2$), 30.1 (q, $C(CH_3)_3$), 20.2 (t, $NHCH_2(CH_2)_2CH_3$), 13.9, 13.7 (q, $N(CH_2CH_3)_2$), 12.8 (q, $NH(CH_2)_3CH_3$); *m*/*z* 1101 $(M + H)^+$ (Found: C, 50.78; H, 9.21; N, 5.18. $C_{68}H_{100}O_8N_4$ requires C, 50.87; H, 9.14; N, 5.08%).

25,27-Bis(*N*,*N*-diethylaminocarbonylmethoxy)-26,28-bis(*N*-butylaminocarbonylmethoxy)calix[4]arene (L6) (partial cone). Pure compound **L6** was obtained by column chromatography (SiO_2: hexane–ethyl acetate = 2 : 8): (yield 23%). Mp 167 °C; δ_H(300 MHz; $CDCl_3$; 300 K) 7.46 (2H, d, J 7.5, ArH *meta*), 7.13 (2H, d, J 7.5, ArH *meta*), 7.10 (1H, t, J 6.0, NH), 7.02 (1H, t, J 7.5, ArH *para*), 6.93 (1H, t, J 7.5, ArH *para*), 6.83 (2H, dd, J 7.1, J 2, ArH *meta*), 6.66 (2H, dd, J 7.1, J 2, ArH *meta*), 6.55 (2H, t, J 7.1, ArH *para*), 5.22 (1H, t, J 5.0, NH), 4.50 (2H, d, J 13.5, OCH_2CONR_2), 4.42 (2H, d, J 13.5, OCH_2CONR_2), 4.40 (2H, d, J 13.0, $ArCH_2Ar$, H_{ax}), 4.25 (2H, d, J 14.5, $ArCH_2Ar$), 4.24 and 4.14 (2H, s, OCH_2CONHR), 3.60 (2H, d, J 14.5, $ArCH_2Ar$), 3.40 (4H, m, $N(CH_2CH_3)_2$), 3.24 (2H, d, J 13.0, $ArCH_2Ar$, H_{eq}), 3.23–3.20 (4H, m, $NHCH_2(CH_2)_2CH_3$), 3.06 (2H, q, J 7.4, $N(CH_2CH_3)_2$), 2.98 (2H, q, J 7.4, $N(CH_2CH_3)_2$), 1.45–1.07 (11H, m, $NHCH_2(CH_2)_2CH_3$, $NHCH_2(CH_2)_2CH_3$),

1.17–1.12 (6H, m, $N(CH_2CH_3)_2$), 0.94 and 0.92 (3H, t, *J* 7.4, $N(CH_2CH_3)_2$), 0.92 (3H, t, *J* 7, $NHCH_2(CH_2)_2CH_3$); δ_C(75 MHz; $CDCl_3$; 300 K) 168.7, 167.8, 166.8 (s, CH_2CON), 155.8 (s, Ar *ipso*), 135.6, 133.8, 133.2, 132.9 (s, Ar *ortho*), 130.8, 129.1, 128.9, 128.5 (d, Ar *meta*), 123.5, 122.5 (d, Ar *para*), 72.3, 71.6, 68.4 (t, OCH_2CO), 41.0 (t, $NHCH_2R$), 40.2, 38.9, 38.5 (t, $N(CH_2CH_3)_2$), 36.5 (t, $ArCH_2Ar$), 31.7 (t, $N(CH_2CH_3)_2$), 31.0 (t, $ArCH_2Ar$), 30.9 (t, $N(CH_2CH_3)_2$), 20.1, 20.0, 14.2, 13.8 (t, $NHCH_2(CH_2)_2CH_3$), 13.6, 12.8 (q, $NH(CH_2)_3CH_3$); *m/z* 878 $(M + H)^+$ (Found: C, 71.09, H, 7.90, N, 6.48. $C_{52}H_{68}O_8N_4$ requires C, 71.21; H, 7.81; N, 6.39%).

Physicochemical measurements

Materials. The solvents methanol (Carlo Erba, max. 0.01% water) and dichloromethane (Carlo Erba, max 0.02% water) were used without any further purification. The supporting electrolyte used in the stability constant determinations, either Et_4NCl (Fluka, purum) or Et_4NClO_4 (Acros) according to the experimental method, was recrystallised twice from doubly-distilled water and dried under vacuum for 24 h at room temperature. The metal salts were chosen according to their solubilities in the solvent: LiCl (Fluka, purum), NaCl (Merck, p.a.), KCl (Merck, p.a.) RbCl (Fluka, puriss.), CsCl (Merck, p.a.), $Mg(ClO_4)_2{\cdot}xH_2O$ (Merck, p.a.), $Ca(ClO_4)_2{\cdot}4H_2O$ (Fluka, purum), $Sr(Cl)_2.6H_2O$ (Aldrich, 99%), $Sr(NO_3)_2$ (Merck, p.a.), $Ba(ClO_4)_2$ (Prolabo, rectapur) and $AgClO_4{\cdot}H_2O$ (Fluka, puriss.) were used for spectrophotometric and potentiometric measurements in methanol. All these salts were dried under vacuum for 24 h before use. The stock solutions of all of them except alkali cations were standardised by complexometric titrations with EDTA in the presence of appropriate coloured indicators.[12] The preparation of all the picrate salts employed in extraction experiments has already been reported.[13]

Picrate extraction measurements. The extraction experiments from water into dichloromethane were performed according to the following procedure: 5 ml of a 2.5×10^{-4} mol dm^{-3} aqueous picrate solution and 5 ml of a 2.5×10^{-4} mol dm^{-3} solution of calixarene in CH_2Cl_2 were mechanically shaken in a stoppered glass tube for 3 min, then magnetically stirred in a thermoregulated water bath at 20 ± 0.1 °C for 30 min and finally left standing for a further 30 min in order to obtain good separation of the two phases. The absorbance *A* of the metal picrates remaining in the aqueous phase was then determined spectrophotometrically at 355 nm. The percentage extraction, %*E*, are derived from the expression $100(A_0 - A)/A_0$, where A_0 is the absorbance of the aqueous solution of a blank experiment without calixarene.

Stability constant measurements. The stability constants β, defined as the concentration ratio $[ML^{n+}]/[M^{n+}]\,[L]$ (where M^{n+} = cation, L = ligand) have been determined in methanol by UV absorption spectrophotometry, at 25 °C and at the ionic strength 0.01 mol dm^{-3}, according to the procedure already described in detail.[4] The ligand concentrations ranged between 10^{-4} and 2.0×10^{-4} mol dm^{-3} and the spectra were treated using the program SIRKO.[14] When the stability constants were too high ($\log \beta > 6.0$), *i.e.* in the case of Na^+, Ca^{2+}, Sr^{2+} and Ba^{2+} with ligand **L1D**, attempts were made to obtain accurate values using competitive potentiometry with Ag^+ as auxiliary cation. Complexation of Ag^+ by this ligand, followed by direct potentiometry, led to the formation of the two following complexes: $Ag(\mathbf{L1D})^+$ with $\log \beta = 6.4 \pm 0.2$ and $Ag_3(\mathbf{L1D})_2^{3+}$ with $\log \beta_{32} = 21.4 \pm 0.4$. Stability constants of the Na^+ and Ba^{2+} 1:1 complexes could be accurately established. However, the competition was not possible for Ca^{2+} and Sr^{2+} which form very stable complexes ($\log \beta \geq 9$).

Calorimetric measurements. The calorimetric determinations were made in methanol at 25 °C, using a precision Isoperibol titration calorimeter (Tronac 450, Orem, Utah). The experimental procedure has been reported in detail elsewhere.[6] The metallic salts ($0.01 \leqslant C_M \leqslant 0.6$ mol dm^{-3}) were titrated into a 50 cm^3 solution of calixarene ($C_L = 7.5 \times 10^{-4}$ mol dm^{-3}). Heat-of-dilution corrections were made by titrating the metal into the solvent. ΔH values were refined from calorimetric data using the program SIRKO.[14] In the case of **L1** complexes of Li^+ and Rb^+, where $\log \beta < 4$, $\log \beta$ and ΔH could be refined simultaneously using the same program. Full agreement was found with spectrophotometric results. Finally $T\Delta S$ was derived from the expression: $\Delta G = \Delta H - T\Delta S$, knowing $\Delta G = -RT \ln \beta$.

Molecular modelling

Molecular dynamics simulations. We used the modified AMBER4.1 software[15] with the representation of the potential energy given in eqn. (1).

$$U = \Sigma_{\text{bonds}} K_r (r - r_{\text{eq}})^2 + \Sigma_{\text{angles}} K_\theta (\theta - \theta_{\text{eq}})^2 + \Sigma_{\text{dihedrals}} \Sigma_n V_n(1+\cos n\varphi) + \Sigma_{i<j} (q_i q_j / R_{ij} - 2\varepsilon_{ij}(R_{ij}^*/R_{ij})^6 + \varepsilon_{ij}(R_{ij}^*/R_{ij})^{12}) \quad (1)$$

The interaction between atoms separated by at least three bonds and those involving their ions are described within a pairwise additive scheme by a 1–6–12 potential. Parameters for the solutes were taken from the AMBER force field[16] and from previous studies on these molecules in pure homogeneous solvents. The atomic charges on **L1** and **L3** are those from ref. 17 and were used without a special scaling factor for 1–4 interactions. The primary amide moiety was adapted from the glycine charges of ref. 18. The Pic^- anion is described in ref. 19. The Sr^{2+} cation is described by the Åqvist parameters.[20] For the solvent, we used the TIP3P model for water[21] and the OPLS models for methanol and for chloroform.[22] A residue based cut-off of 12 Å was used for the non-bonded interactions.

The simulated solvent systems are described in Table 1. The water/chloroform interface has been built as indicated in ref. 23. After immersion of the solute, each system was energy minimized (1000 steps). Then the MD simulations were started with random velocities, and the temperature was controlled at 300 K by coupling to a thermal bath with a relaxation time of 0.2 ps. All C–H, O–H, H···H, C–Cl and Cl···Cl "bonds" were constrained with SHAKE, using a time step of 1 fs.

Quantum mechanics. The QM calculations were performed on **A** free, **A**/Na^+, **A**/Sr^{2+} and **A**/Eu^{3+} complexes (**A** = amide: DMA, MA-*cis* and -*trans* and AA; see Scheme 1) at the SCF HF level using the Gaussian94 program.[24]

The D95 double-zeta basis set was used for **A**. For the Na^+ ion, we used the 6–31G* basis set.[24] The Sr^{2+} ion was described by a pseudo-potential for the 28 ([Ar] + $3d^{10}$) core electrons, and explicit 4s, 4p and 5s orbitals, described by a (6s,6p,5d)/[4s, 4p,2d] basis set from ref. 25. The 46 + $4f^n$ core electrons of the Eu^{3+} cation were represented by the quasi-relativistic pseudo-potential of Dolg *et al.*[26] and the valence electrons by a (7s,6p,5d)/[5s,4p,3d] gaussian basis set supplemented by one *f* polarization function of exponent 0.591. Geometry optimizations of the position of Na^+, Sr^{2+} or Eu^{3+} cations, and of C=O and C–N distances were carried out numerically, keeping the other parameters of **A** frozen at their values optimized in **A** free. The cation–ligand interaction energies ΔE were calculated as the difference between the energy minimized structures of the free and complexed ligand **A**, and corrected for basis set superposition errors (BSSE) (ΔE_{cor}).[27]

Table 1 Simulation conditions in solution

		Solvent	Box size/Å	Number of solvent molecules	Simulation time/ns
L1	$Sr(Pic)_2$	Interface	49 × 39 × 60	420 + 1830	1
	$Sr(Pic)_2$	$CHCl_3$	51 × 41 × 39	566	0.3
L3	—	Gas	—	—	0.2
	$2O_c \cdots HN^a$	$CHCl_3$	40 × 38 × 37	394	0.5
	$2O_e \cdots HN^b$	$CHCl_3$	42 × 39 × 39	432	0.5
	No $O \cdots HN^c$	$CHCl_3$	41 × 40 × 37	410	0.5
	$2O_c \cdots HN^a$	MeOH	40 × 38 × 38	789	0.5
	$2O_e \cdots HN^b$	MeOH	41 × 40 × 37	843	0.5
	No $O \cdots HN^c$	MeOH	41 × 40 × 37	821	0.5
L3	$Sr(Pic)_2$	MeOH	52 × 41 × 38	1107	0.3
	$Sr(Pic)_2$	$CHCl_3$	51 × 41 × 38	560	0.5
	$Sr(Pic)_2$	Interface	49 × 39 × 60	417 + 1829	1

[a] O_c = carbonyl oxygen. Two $O_c \cdots HN$ hydrogen bonds at the beginning of the simulation. [b] O_e = ether oxygen. Two $O_e \cdots HN$ hydrogen bonds at the beginning of the simulation. [c] No hydrogen bond at the beginning of the simulation.

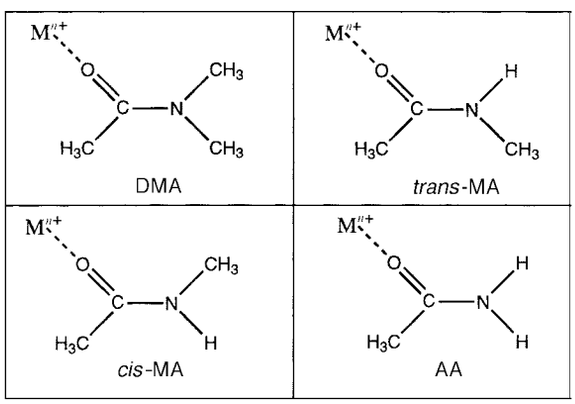

Scheme 1 The DMA, MA and AA complexes of Na^+, Sr^{2+} and Eu^{3+} (*ab initio* QM calculations).

Results

Synthesis of the ligands

The synthesis of **L3** and **L4** bearing mixed tertiary and primary amide groups at the lower rim of the calix[4]arenes and **L5** and **L6** bearing tertiary and secondary amides was carried out by alkylation of the previously reported 1,3-bis(*N*,*N*-diethylaminocarbonylmethoxy)calix[4]arene (**I** or **II**),[7] with the proper α-chloroacetamide (Scheme 2).

We first used NaH as base and dry DMF as solvent, since these are usually the best conditions to block the calixarene in the cone conformation,[28] but mixtures of byproducts were obtained, some of them resulting also from the alkylation of amidic NH functions. The use of a milder base, K_2CO_3, in dry acetone gave products **L3**–**L6** in yields ranging from 20 to 72%. Under these conditions the stereochemical outcome of the reaction depends on the alkylating agent and the starting calixarene. When *tert*-butyl groups were present at the upper rim of the calixarene only products in the cone conformation (**L3** and **L5**) were obtained. On the contrary, the dealkylated bisamide (**II**) gave ligand **L6** in the partial cone, and **L4** in a mixture of cone and 1,3-alternate conformations. The structural assignment for these ligands was made on the basis of the ^1H and ^{13}C NMR spectral analysis of the signals of the $ArCH_2Ar$ groups.[29] In ligand **L6** these groups give two AX systems (δ 4.25 and 3.60, J = 14.5 Hz; δ 4.40 and 3.24, J = 13.0 Hz) of four protons each, whereas in ligand **L4** they give AB (δ 3.97 and 3.70, J = 15.6 Hz) and AX (δ 4.56 and 3.27, J = 13.8 Hz) systems which are in a ratio 1:2, indicating the presence of the cone and 1,3-alternate structures in the same proportion.

^1H NMR studies

In order to correlate the structural properties of ligand **L3** and its binding ability towards strontium cation, in different solvents, we have performed ^1H NMR experiments on the free ligand **L3** and its strontium picrate complex, both in $CDCl_3$ and CD_3OD. Interestingly, the ^1H NMR spectrum of **L3** in $CDCl_3$ shows two distinct and sharp singlets for the NH_2 protons at δ 8.36 and 6.10 which do not change significantly upon dilution, suggesting that one of the two NH groups is intramolecularly hydrogen bonded in chloroform solutions. Moreover, the presence of two distinct and quite separate singlets for the aromatic protons at δ 7.12 and 6.56 and for the *tert*-butyl groups at δ 1.33 and 0.85 indicates that the ligand possesses a C_{2v} structure in solution which is typical of the flattened cone conformation of tetraalkoxycalix[4]arenes.

The correlation peaks present in the ROESY map between the two quartets of NCH_2CH_3 protons at δ 3.43 and 3.13, the singlet of the $OCH_2CON(CH_2CH_3)_2$ at δ 4.36, and the ArH signal at δ 6.56, indicate that the two aromatic nuclei bearing the tertiary amide groups are parallel to each other, while the aromatic nuclei having the CH_2CONH_2 functions are more perpendicular, in agreement with molecular modeling studies (*vide infra*). In CD_3OD solution, the conformation of **L3** is still a C_{2v} flattened cone, but nothing can be said about hydrogen bonding since the NH_2 protons exchange with deuterium of the solvent and are not visible in the spectrum (Fig. 1(a)).

Upon titration of this solution with a $SrPic_2$ (strontium picrate) CD_3OD solution the signals of the complex appear in the spectrum together with those of the free ligand until the ratio M/L < 1, thus indicating that the exchange of the cation is slow on the ^1H NMR time-scale (Fig. 1(b)). When M/L reaches a value of 1 (Fig. 1(c)), the signals of the free ligand **L3** disappear and the spectrum remains unchanged even after adding more strontium picrate solution.

This experiment shows that the complex has a 1:1 stoichiometry. Its ^1H NMR spectrum (Fig. 1(c)) shows the two singlets of the ArH (δ 7.39 and 7.40) and of the *tert*-butyl groups (δ 1.20 and 1.19) very close each to the other, which indicates that the conformation of the calixarene becomes more symmetrical, close to a regular cone. We also studied the **L3**Sr^{2+} complex in chloroform solution. To prepare this complex, we stirred overnight a $CDCl_3$ solution of **L3** with an excess of solid $SrPic_2$ and filtered the undissolved salt. Surprisingly the ^1H NMR spectrum of this complex is very different from that recorded in CD_3OD.

All protons were assigned using two-dimensional COSY and ROESY experiments and the data are reported in Table 2 and Fig. 2. The ArH protons give four doublets (J = 2–4 Hz) between δ 7.13 and 6.27 while the methylene protons of the

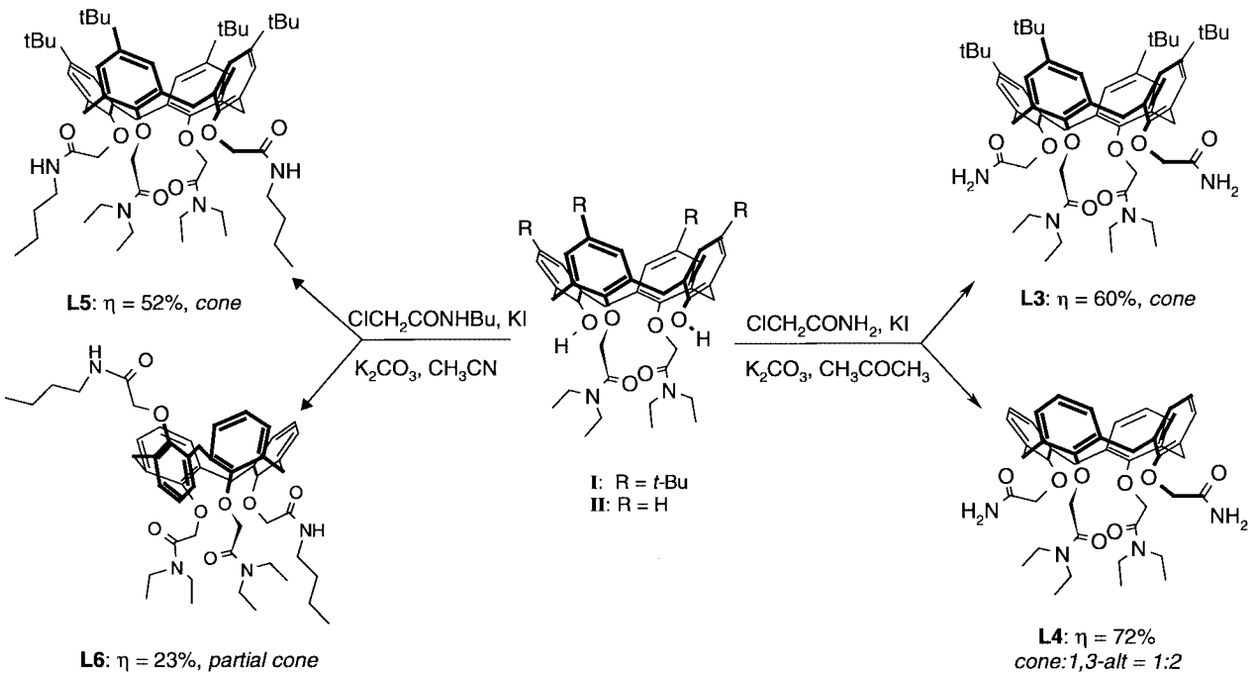

Scheme 2 Synthesis of the ligands.

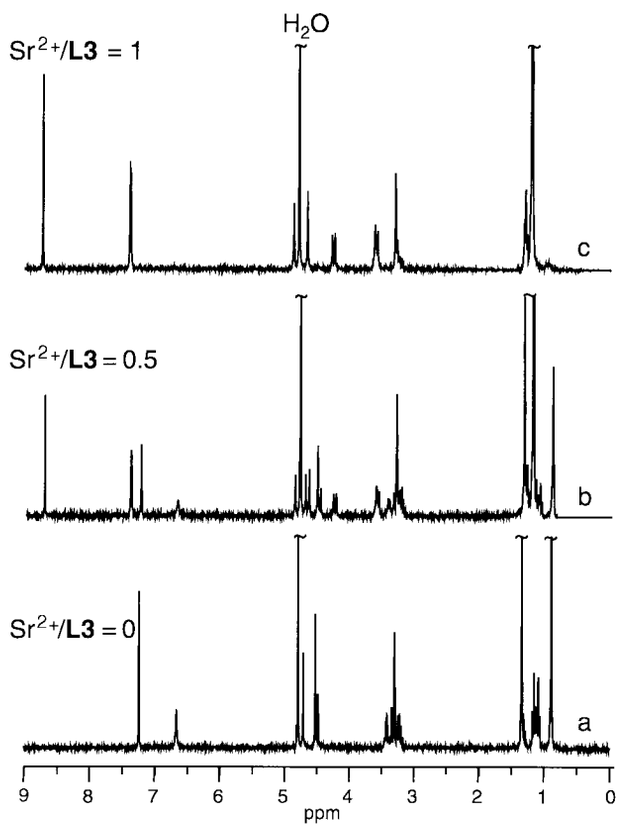

Fig. 1 ^{1}H NMR spectra (CD_3OH, 300 MHz, 300 K) of (a) compound **L3**, (b) compound **L3** with 0.5 equiv. of $SrPic_2$, (c) compound **L3** with 1.0 equiv. of $SrPic_2$.

bridge ($ArCH_2Ar$) and those α to the amide groups give eight doublets between δ 6.08 and 2.52. This indicates that the Sr^{2+} complex possesses only a C_2 symmetry axis. Further information on the structure of this complex can be obtained by observing several differences between the spectrum of the complex and that of the free ligand. It is worth noting that protons A and B of the $ArCH_2Ar'$ methylene group, E and F of the Ar′ aromatic ring and Q of the *tert*-butyl group are all substantially shifted to higher field, whereas one of the diastereotopic protons (C) of the OCH_2CONH_2 chain is remarkably shifted downfield. This could be due to the presence of the picrate anions, which form a tight ion pair in $CDCl_3$ and are unsymmetrically located close to the Ar′ nuclei, disrupting the C_{2v} symmetry of the free ligand **L3**.

Table 2 Chemical shifts (ppm) of the free ligand **L3** and its strontium picrate (**L3**$SrPic_2$) complex in $CDCl_3$ at room temperature

Proton	δ in free **L3**	δ in **L3**$SrPic_2$
picrate	—	8.87
O, P	8.36, 6.10	8.57, 7.83
H	6.56	7.14
G	6.56	6.78
F	7.12	6.43
E	7.12	6.27
C	4.81	6.08
D	4.81	4.69
M/N	4.36	4.37
L	4.46	4.26
B	4.46	3.99
N/M	4.36	3.85
I	3.25	3.32
NCH_2CH_3	3.43, 3.14	3.9–3.8, 3.35–3.00
A	3.25	2.52
R	0.85	1.36
NCH_2CH_3	1.19–1.11	1.25–1.19, 1.14–1.10
Q	1.33	0.79

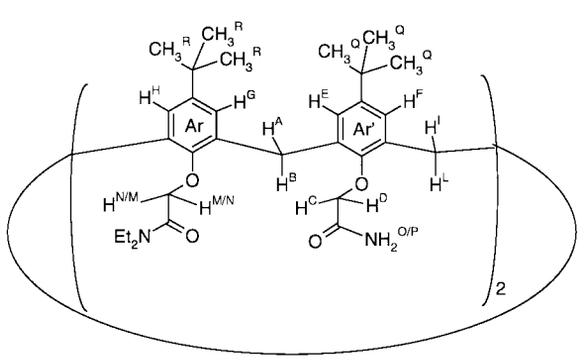

Fig. 2 Proton assignment of the **L3**$Sr(Pic)_2$ complex in $CDCl_3$.

Table 3 Percentage extraction (%E)[a] of alkali and alkaline-earth picrates from H_2O into CH_2Cl_2 at 20 °C

Ligands	Li^+	Na^+	K^+	Rb^+	Cs^+	Mg^{2+}	Ca^{2+}	Sr^{2+}	Ba^{2+}	Ag^+
L1[b]	63	95.5	74	24	12	9	98	86	74	—
L2[c]	<1	2.7	<1	5.2	3.1	<1	5.8	4.6	4.8	—
L1D	36.5 ± 0.8	90.3 ± 0.8	52.2 ± 0.2	11.7 ± 0.8	5.8 ± 0.5	4.5 ± 0.5	79.0 ± 0.4	56.5 ± 0.3	43.0 ± 0.1	90.0 ± 0.2
L3	3.8 ± 0.2	4.6 ± 0.6	4.0 ± 0.1	6.6 ± 0.2	4.0 ± 0.1	2.0 ± 0.1	5.6 ± 0.2	3.2 ± 0.3	2.6 ± 0.1	6.2 ± 0.6
L4	1.1 ± 0.1	3.3 ± 0.5	8.1 ± 0.3	5.3 ± 0.4	2.1 ± 0.1	≤1	2.6 ± 0.1	≤1	≤1	31.8 ± 0.9
L5	13.4 ± 0.6	22.0 ± 0.4	14.1 ± 0.2	16.2 ± 0.4	12.0 ± 0.9	9.9 ± 0.2	30.1 ± 0.3	16.5 ± 0.8	9.9 ± 0.1	21.7 ± 0.7
L6	≤1	1.5 ± 0.1	≤1	≤1	≤1	≤1	≤1	≤1	≤1	14.5 ± 0.1

[a] Arithmetic mean of at least three independent experiments. [b] Ref. 4. [c] Ref. 7.

Table 4 Stability constant (log $\beta \pm \sigma_{n-1}$)[a] of alkali and alkaline-earth complexes in methanol at 25 °C, I = 0.01 mol dm^{-4}

Ligands	Li^+	Na^+	K^+	Rb^+	Cs^+	Mg^{2+}	Ca^{2+}	Sr^{2+}	Ba^{2+}
L1[b]	4.1	7.9	5.8	3.8	2.5	—	≥9	≥9	7.2
L3	≤1	3.3 ± 0.1[c]	≤1	≤1	≤1	1.5 ± 0.1[c]	6.0 ± 0.2[c]	5.4 ± 0.2[c]	3.3 ± 0.1[c]
L4	≤1	2.9 ± 0.2[c]	4.1 ± 0.1[c]	3.6 ± 0.1[c]	1.9 ± 0.4[c]	1.1 ± 0.2[c]	5.9 ± 0.3[c] 9.7 ± 0.1[d]	4.4 ± 0.3[c]	2.5 ± 0.1[c]
L5	≤1	>6[c]	2.3 ± 0.1[c]	≤1	≤1	≤1	>6[c]	>6[c]	3.7 ± 0.3[c]
L6	≤1	2.1 ± 0.1[c]	2.2 ± 0.1[c]	≤1	≤1	≤1	≤1	≤1	≤1

[a] Arithmetic means of n independent experiments; precision: $\pm\sigma_{n-1}$, = standard deviation on the means. [b] Ref. 4. [c] Spectrophotometric measurements. [d] Corresponding to $Ca^{2+} + 2\mathbf{L4} \rightleftharpoons Ca\mathbf{L4}_2^{2+}$.

Table 5 Thermodynamic parameters of complexation[a] of alkali and alkaline-earth complexes with **L1D** and **L1** in methanol at 25 °C

Ligands		Li^+	Na^+	K^+	Rb^+	Cs^+	Mg^{2+}	Ca^{2+}	Sr^{2+}	Ba^{2+}
L1D	log β	3.0 ± 0.1[b]	7.2 ± 0.1[c]	5.0 ± 0.1[d]	2.0 ± 0.1[b]	≤1	≤1[d]	≥9[c]	≥9[c]	6.53 ± 0.03[c]
	$-\Delta G$	17.1 ± 0.6	42.2 ± 0.6	28.5 ± 0.6	11.4 ± 0.6	nd	—	≥51.3	≥51.3	36.4 ± 0.2
	$-\Delta H$	1 ± 1	41 ± 1	33.3 ± 0.4	27 ± 2	—	—	29 ± 1	13.6 ± 0.9	8.2 ± 0.3
	$T\Delta S$	16 ± 2	1 ± 2	−5 ± 1	−16 ± 3	—	—	≥22.3	≥37.7	28.2 ± 0.5
L1[e]	log β	4.1	7.9	5.8	3.8	2.5	1.2	≥9	≥9	7.2
	$-\Delta G$	22.2	45	33.1	21.6	14	—	≥51.3	≥51.3	41
	$-\Delta H$	7	50.6	42.4	17.5	9	—	25	10	−2.5
	$T\Delta S$	15	−6	−9.3	4	5	—	≥26.3	≥41.3	43

[a] In kJ mol^{-1}. [b] Mean spectrophotometric and calorimetric measurements. [c] Potentiometric measurements. [d] Spectrophotometric measurements. [e] Ref. 6.

Extraction and complexation data

Extraction data reported in Table 3 show that the replacement of two distal tertiary amides of the *p-tert*-butylcalix[4]arene tetrakis(diethylamide) **L1** by secondary amides as in **L5** leads to a dramatic decrease of the extraction percentages of most alkali and alkaline-earth picrates. For instance there is a drop of *ca*. 73 and 68% on the extraction levels of $Na^+$and Ca^{2+}, respectively. However, in both series of cations, the selectivity profiles remain in favour of Na^+ and Ca^{2+} as for compound **L1**. An even more important decrease is observed with compound **L2** bearing four *N*-butylamide functions. The introduction of two primary amides as in **L3** further decreases the extraction levels (%$E \leq 7$%) and the selectivity.

Compound **L6** devoid of *tert*-butyl groups in the *para* position and possessing a partial cone conformation is a totally inefficient ligand except for silver picrate, which is moderately extracted (%E = 14%).

Very low extraction levels have also been found with the *para*-dealkylated ligand **L4**, with however a slight selectivity for K^+ (%E = 8), which may be due to the presence in this compound of about 70% of the 1,3-alternate conformer. Tetramers in the 1,3-alternate conformation are well known to display a high affinity for this cation.[30]

Complexation data for alkali and alkaline-earth metal ions are given in Table 4. In line with extraction data, the replacement of two tertiary amides of **L1** by secondary amides (compound **L5**) leads to a substantial decrease of the stability of the complexes, although the stability of the Na^+ complex is still high (log β > 6). In this case no competition experiments with Ag^+ could be performed because of precipitation occuring during titration in the presence of this cation, preventing an accurate determination of the stability. However the decrease in stability is clearly indicated for the potassium complex (log β = 2.3 instead of 5.8 with **L1**) and for the other complexes (log $\beta \leq 1$).

The replacement of the secondary amides by primary amides (**L3**) still decreases the stability constants and the only one which could be determined is log β = 3.3 for the Na^+ complex. It can be noted that, if the complexation level appears to be strongly dependent on the nature of the amide groups and decreases from the tertiary to the secondary and to the primary according to the basicity of the carbonyl oxygen atoms, the selectivity still remains in favour of Na^+. The same trends can be observed within the alkaline-earth metals, the preference being towards Ca^{2+} and Sr^{2+} in this series of cations. This results in high Sr^{2+}/Na^+ and Ca^{2+}/Na^+ selectivities of *ca*. 500 and 125, respectively. Moreover, it must be emphasized that, if ligand **L3** is a very good binder for Ca^{2+} and Sr^{2+} in methanol (log β = 6.0 and 5.4, respectively), it is a very poor extractant for the corresponding picrates (%E = 5.6 and 3.2).

Ligand **L6** in the partial cone conformation is totally inefficient towards alkali and alkaline-earth metals, except Na^+ and K^+, with which it forms complexes of rather low stability (log $\beta \approx 2$). However, it complexes Ag^+ more strongly (log β = 3.6).

Results obtained for the *para*-H counterpart of compound **L1** (**L1D**) show a substantial decrease of stability upon dealkylation, ranging from 0.5 and 1.8 log units in the case of the alkali cations (Table 4).

Calorimetric results, given in Table 5, show that complex-

Table 6 Interaction energies, optimised structures and Mulliken charges in amide-X,Y free ligands and in their complexes

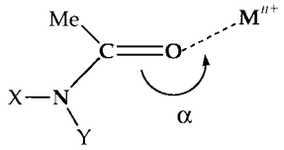

			Interaction energies	Optimized distances (Å) and angles (°)				Mulliken charges						
X	Y	M^{n+}	$\Delta E/\Delta E_{cor}$ [a]	$d(M^{n+}\cdots O)$	d(C=O)	d(C–N)	α	q(M)	q(O)	q(C)	q(N)	q(Me)	q(X)	q(Y)
H	H	(none)	—	—	1.231	1.369	—	—	−0.44	0.50	−0.81	−0.01	0.36	0.39
		Na^+	−46.8/−45.5	2.070	1.255	1.339	185	0.91	−0.67	0.61	−0.76	0.09	0.41	0.41
		Sr^{2+}	−95.5/−94.3	2.224	1.289	1.317	185	1.85	−0.84	0.68	−0.72	0.15	0.45	0.43
		Eu^{3+}	−200.9/−198.8	2.015	1.350	1.293	186	2.62	−0.95	0.73	−0.64	0.27	0.50	0.46
H	Me	(none)	—	—	1.234	1.363	—	—	−0.46	0.53	−0.61	−0.03	0.36	0.21
		Na^+	−48.1/−46.8	2.064	1.259	1.335	187	0.90	−0.68	0.63	−0.55	0.05	0.40	0.24
		Sr^{2+}	−98.9/−97.7	2.213	1.292	1.314	186	1.84	−0.87	0.71	−0.51	0.12	0.44	0.27
		Eu^{3+}	−209.4/−207.3	2.004	1.352	1.291	187	2.60	−0.95	0.72	−0.42	0.23	0.49	0.33
Me	H	(none)	—	—	1.235	1.367	—	—	−0.46	0.49	−0.59	−0.00	0.18	0.38
		Na^+	−49.3/−48.0	2.060	1.263	1.335	186	0.90	−0.67	0.59	−0.55	0.08	0.25	0.40
		Sr^{2+}	−101.7/−100.4	2.209	1.300	1.312	186	1.84	−0.87	0.67	−0.51	0.15	0.32	0.41
		Eu^{3+}	−214.8/−212.5	2.001	1.364	1.289	187	2.59	−0.96	0.71	−0.44	0.26	0.41	0.43
Me	Me	(none)	—	—	1.238	1.369	—	—	−0.48	0.53	−0.39	−0.02	0.17	0.19
		Na^+	−50.0/−48.6	2.057	1.267	1.337	190	0.90	−0.70	0.63	−0.34	0.06	0.24	0.22
		Sr^{2+}	−104.1/−102.8	2.200	1.303	1.315	188	1.83	−0.90	0.70	−0.31	0.12	0.30	0.25
		Eu^{3+}	−222.8/−220.6	1.988	1.370	1.292	188	2.56	−0.96	0.71	−0.23	0.22	0.39	0.31

[a] Interaction energies (kcal mol^{-1}) without/with BSSE correction (1 kcal = 4.18 kJ).

ation of Na^+, K^+ and Rb^+ is enthalpy controlled: ΔH values are strongly negative but however less negative than with those found with the *p-tert*-butyl counterpart **L1**. This can be related to the greater conformational mobility of **L1D** and to its greater solvation. The corresponding entropy changes are similar or slightly less negative than with **L1**. On the contrary, the stabilization of the small and highly solvated Li^+ cation is entropy driven, as already observed with **L1**. The decrease in stability upon dealkylation thus results from a decrease in enthalpy, which is not compensated by an increase in entropy. Moreover the dealkylation does not affect the trends observed in the series, *i.e.* an exothermic maximum for Na^+. However, the minimum of entropy is observed for Rb^+ instead of K^+. The entropy changes should be mainly related to the ligand solvation among other factors, since dealkylation does not produce any change in $T\Delta S$ with the most solvated Li^+ cation.

With alkaline earth cations, no definite conclusions could be drawn as only lower limits for ΔG and hence for $T\Delta S$ could be obtained. However, it can be seen that dealkylation affects ΔH values which surprisingly become more favourable with **L1D**, especially for Ba^{2+}.

Molecular modeling results

Intrinsic binding features of primary/secondary/tertiary amides. According to the QM calculations on the model sytems (Scheme 1 and Table 6), the interaction energy between the Na^+, Sr^{2+}, Eu^{3+} cations and amides increases in the sequence: primary (AA) < secondary-*cis* (MA-*cis*) < secondary-*trans* (MA-*trans*) < tertiary (DMA) amides. Thus, for the Sr^{2+} cation, interactions relative to the primary amide AA increase with secondary (by 3.4 kcal mol^{-1} for MA-*cis* and 6.2 kcal mol^{-1} for MA-*trans*) and tertiary amides (by 8.6 kcal mol^{-1} for DMA). With Na^+ as cation, the difference between primary and tertiary amides is smaller (3.2 kcal mol^{-1}), while with Eu^{3+} it is larger (28.9 kcal mol^{-1}; Table 6).

These trends correlate with the increased charge transfer to the cation in the series (0.09 to 0.10 e for Na^+, 0.15 to 0.17 e for Sr^{2+} and 0.38 to 0.44 e for Eu^{3+}) and with polarization of the $O^{\delta-}-C^{\delta+}-N^{\delta-}-X^{\delta+}$ moiety by the cation (X = Me/H, *trans* to O=C). As expected, enhanced polarization of the amide and stabilization of the complex are found when X = alkyl, compared to H. They are also enhanced when the hardness of the cation increases (compare Eu^{3+} to Sr^{2+} and Na^+; Table 6).

The structural features ($M^{n+}\cdots O$, O=C and C–N distances) are fully consistent with the stabilization of the resonant form of the amide (Scheme 3) by alkyl, compared to H groups: the

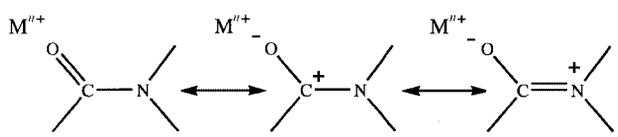

Scheme 3 Schematic representation of stabilizing electronic effects on the $M^{n+}\cdots$ amide complexes.

stronger the binding, the shorter are the $M^{n+}\cdots O$ and C–N distances, and the longer is the O=C distance.

This also explains why the *trans* complex of secondary amides is more stable than the *cis* one. In all complexes, we notice that the cation is not exactly aligned with the C=O axis, but slighty *trans* to the C–N bond.

The calculations point out the importance of intrinsic interactions between primary/secondary/tertiary amides with a given cation, in their optimized geometry. In the calix[4]arene complexes, these interactions may differ, as the cation position with respect to the four amide groups is not optimal. Effective interactions also depend on the solvent (see next).

The question of internal hydrogen bonding in the mixed amide ligand L3. As the NMR spectrum of **L3** indicates hydrogen bonding with NH_2 protons in chloroform, we simulated **L3** in chloroform and in methanol to determine which structures involve such H-bonds, and also to what extent a protic solvent may compete with these bonds. Three simulations of 500 ps starting with different conformers (*a* to *c*) were performed in each solvent (Table 1): *a* and *b* display initially internal H-bonds, while *c*, (extracted from the Sr^{2+} complex) has none. In *a* the two $NH\cdots O_{amide}$ "bonds" involve oxygens of the $CONEt_2$ branch, while in *b*, the two $NH\cdots O_{ether}$ bonds involve two NH_2 groups and the same O_{ether} oxygen of a $CONEt_2$ branch. The

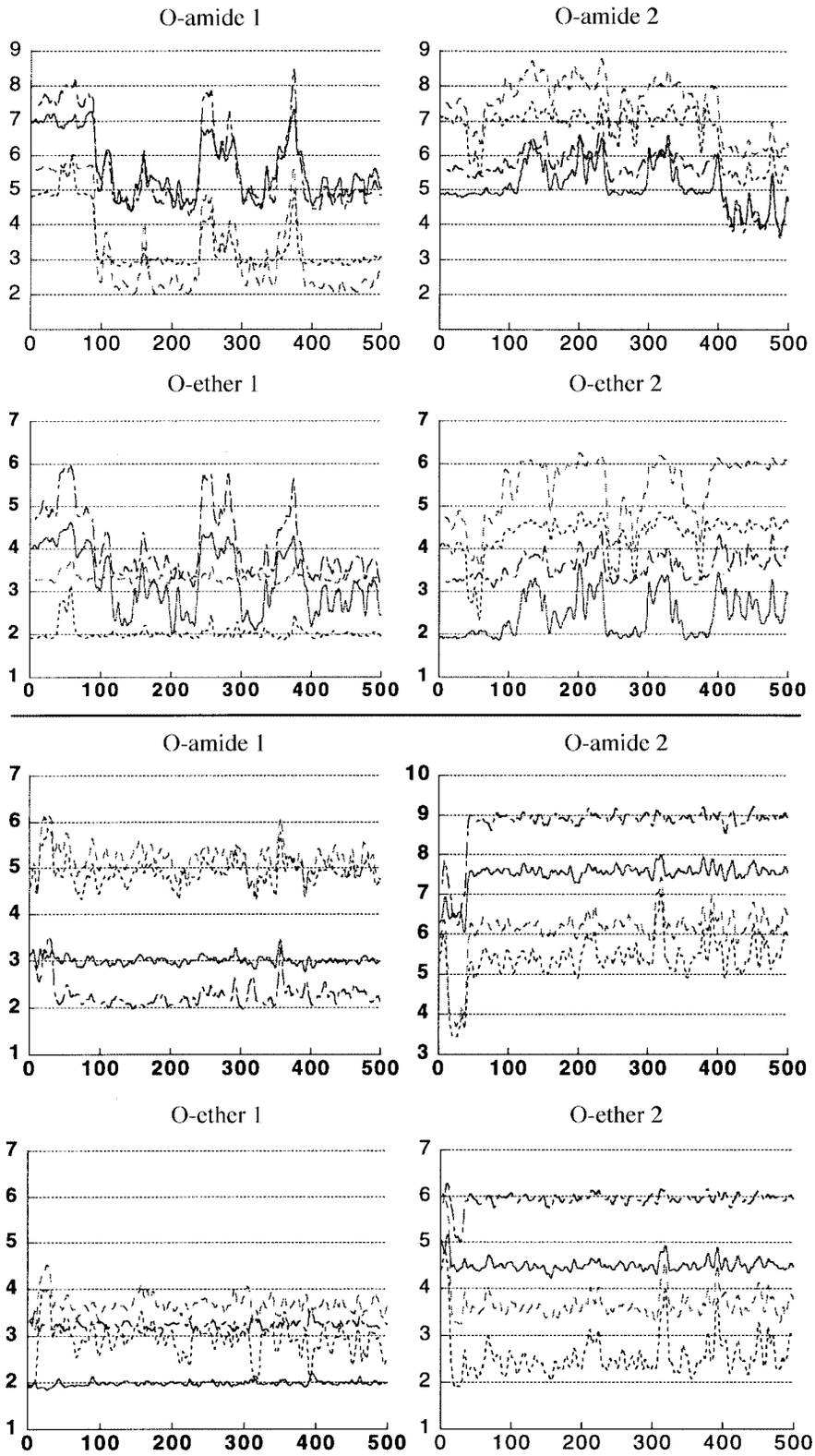

Fig. 3 Simulation of **L3** in chloroform (top) and methanol (bottom). Distances (Å) NH···O_{ether} and NH···O_{amide} as a function of time (ps) (Simulation *b*).

time evolution of these NH···O_{amide} and NH···O_{ether} distances is shown in Fig. 3.

Despite the relatively long simulations (500 ps each) no convergence to a unique type of structure was observed, suggesting that there is no strong driving force for evolving to a marked energy minimum. Each simulation led to a different set of trajectories and conformers, which all displayed short NH···O contacts. However, the patterns were different, and solvent dependent. We considered three criteria to define "internal H-bonds". First, the NH···O distance, which is about 2 Å or less. According to this criteria, H-bonds were present in simulations *a* to *c* and in the two solvents, involving either O_{ether} or O_{amide} oxygens. Hydrogen bonding requires also stereochemical features. In the case of carbonyl amides, NH sits preferentially along the sp^2 oxygen lone pair direction.[31,32] Linear C=O···H–N arrangements are less stable. According to this criteria, no H-bonding to carbonyls was found. NH bonds to O_{ether} oxygens are more flexible than around O_{amide}.[31,32] and were found in

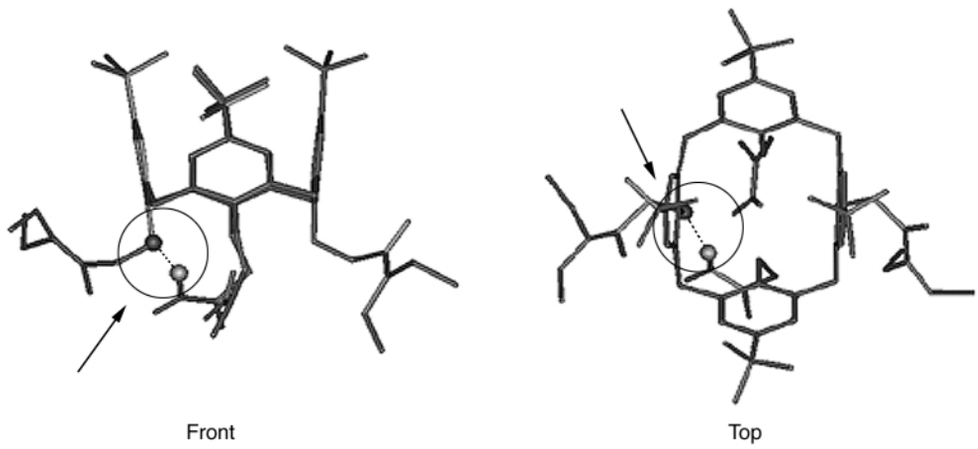

Fig. 4 Snapshots of the free ligand **L3** simulated in chloroform. Typical conformer with one internal NH · · · O_{ether} hydrogen bond.

Table 7 Average Sr^{2+} · · · O distances in the $Sr(Pic)_2$ complexes (X-ray structure) and in **L3**$Sr(Pic)_2$ complexes simulated in chloroform, methanol and at the water/chloroform interface

		Sr^{2+} · · · O_{amide}/Å	Sr^{2+} · · · O_{ether}/Å	ω_{1-3}(°)[a]	ω_{2-4}(°)[a]
L1$Sr(Pic)_2$	X-Ray[b]	2.50 ± 0.01	2.58 ± 0.01	49	43
L3$Sr(Pic)_2$	$CHCl_3$	(2.48[c]/2.44[d]) ± 0.07	2.44 ± 0.06	47.5 ± 0.2	46.8 ± 0.1
L3$Sr(Pic)_2$	MeOH	2.47 ± 0.07	2.43 ± 0.05	47.8 ± 0.2	47.8 ± 0.1
L3$Sr(Pic)_2$	Interface	2.50 ± 0.05	2.52 ± 0.05	47.0 ± 0.1	47.8 ± 0.1

[a] Angles between opposite aromatic cycles. [b] Ref. 17. [c] Sr^{2+} · · · O_{CONE_2} distances. [d] Sr^{2+} · · · O_{CONH_2} distances.

simulations *a* (in chloroform) and *b* (in both solvents). The third criteria is energy. Conformers with internal H-bonding are expected to be more stable than others without H-bonding. In all cases, we found the average energy differences of **L3** in solution to be relatively small (about 5 kcal mol^{-1}, or less), and less than the differences in solute–solvent interaction energies $E_{L3-solv}$ (up to 10 kcal mol^{-1}). Thus, the energy criteria did not reveal any marked stabilization of structures with short NH · · · O contacts.

To summarize, in both solvents we observe some NH · · · O interactions at 2 Å, but they do not all correspond to H-bonds. In no case has the NH · · · O_{amide} moiety the correct orientation. Concerning NH · · · O_{ether} interactions which are less directional, distances are consistent with H-bonds, but energy stabilization occurs only in chloroform for cases *a* and *b*. A typical structure is displayed in Fig. 4. Such NH · · · O_{ether} interactions have been characterized by X-ray analysis of an analogue of **L3**.[33] They may also occur with secondary C(O)NHR amides where the NH proton points to the O_{ether} oxygen, while the NR group points to the solvent. We notice that the cone fragment has nearly C_{2v} symmetry, where the two anisole rings bearing the $CONEt_2$ arms are parallel to each other (ω angle of 10 ± 5°), while those bearing the $CONH_2$ arms are nearly orthogonal (ω angle of 80–100 ± 5°). Although the NH · · · O_{ether} interactions lead to the non-equivalence of the amidic arms on the timescales simulated (500 ps), the latter likely exchange and become equivalent on the NMR timescale.

The L3 $SrPic_2$ complex simulated in chloroform and methanol solutions. According to the MD simulations, the binding mode of Sr^{2+} by **L3** in dry chloroform or in methanol solutions is quite similar to the one for **L1** obtained previously from simulations as well as in the solid state.[17] The Sr^{2+} cation sits in the pseudo-cavity delineated by the four carbonyls and four phenolic oxygens. In methanol and in choloroform, it is nearly equidistant from the four O_{ether} oxygens and from the four O_{amide} oxygens (Table 7). These distances are similar to those obtained in the solid state structure of the **L1**$Sr(Pic)_2$ complex (Table 7).

The four carbonyl groups display a somewhat "tangential", instead of "linear" coordination to the cation (Fig. 5). The cone of the **L3** complex has an average C_{4v} symmetry. The ω angle between the two pairs of opposite phenolic rings is the same (47°) in both solvents, and close to the value found in the solid state (Table 7). Interestingly, depending on the solvent, the two Pic^- anions display distinct relationships with respect to the **L3**Sr^{2+} complex. At the beginning of the simulation (0 ps), they were placed as in the solid state structure of the **L1**$Sr(Pic)_2$ complex, perpendicular to the C_2 symmetry axis of the system.[17] In chloroform solution, they moved somewhat toward the two $CONH_2$ groups, where they remained hydrogen bonded, retaining, on the average, a C_2 symmetry relationship (Fig. 5). This lowers the symmetry of the whole complex, as observed by NMR. In methanol solution, one of the two $CONH_2$ protons is somewhat hydrogen bonded to the solvent while the two Pic^- anions display "π-stacking interactions" with the two $CONEt_2$ substituted phenolic groups (Fig. 5). As a result, the **L3**Sr^{2+} complex is more C_{2v}-like in methanol than in chloroform, in agreement with the NMR data.

Interfacial behaviour of the $SrPic_2$ complexes of L1/L3. The $SrPic_2$ complexes of **L1** and **L3**, simulated at the water/chloroform interface, reveal distinct behaviour, which shows that the complex with **L3** is more surface active and hydrophilic, compared to the **L1** complex. Both simulations started with an inclusive Sr^{2+} complex, equally shared between the two liquid phases (Fig. 6), flanked by the two Pic^- counterions at the interface.

During 1 ns of dynamics simulations, both rotate somewhat, in such a way that the lipophilic *tert*-butyl groups at the upper rim move on the chloroform side, and the lipohilic Sr^{2+} amidic moieties move on the water side. The **L3** complex orientates rapidly perpendicular to the interface, while the **L1** complex is more tilted. It is noticeable that the Sr^{2+} ion of the **L3** complex sits on the water side of the interface, while the Sr^{2+} of the **L1** complex sits on the chloroform side (at 1.6 and −1.2 Å, respectively, from the interface, on average during the last 100 ps). As a result, the **L3**$SrPic_2$ complex interacts much more with water than the **L1**$SrPic_2$ complex (−242 *versus* −200 ± 13 kcal mol^{-1}), mostly due to the contribution of the complexed Sr^{2+}

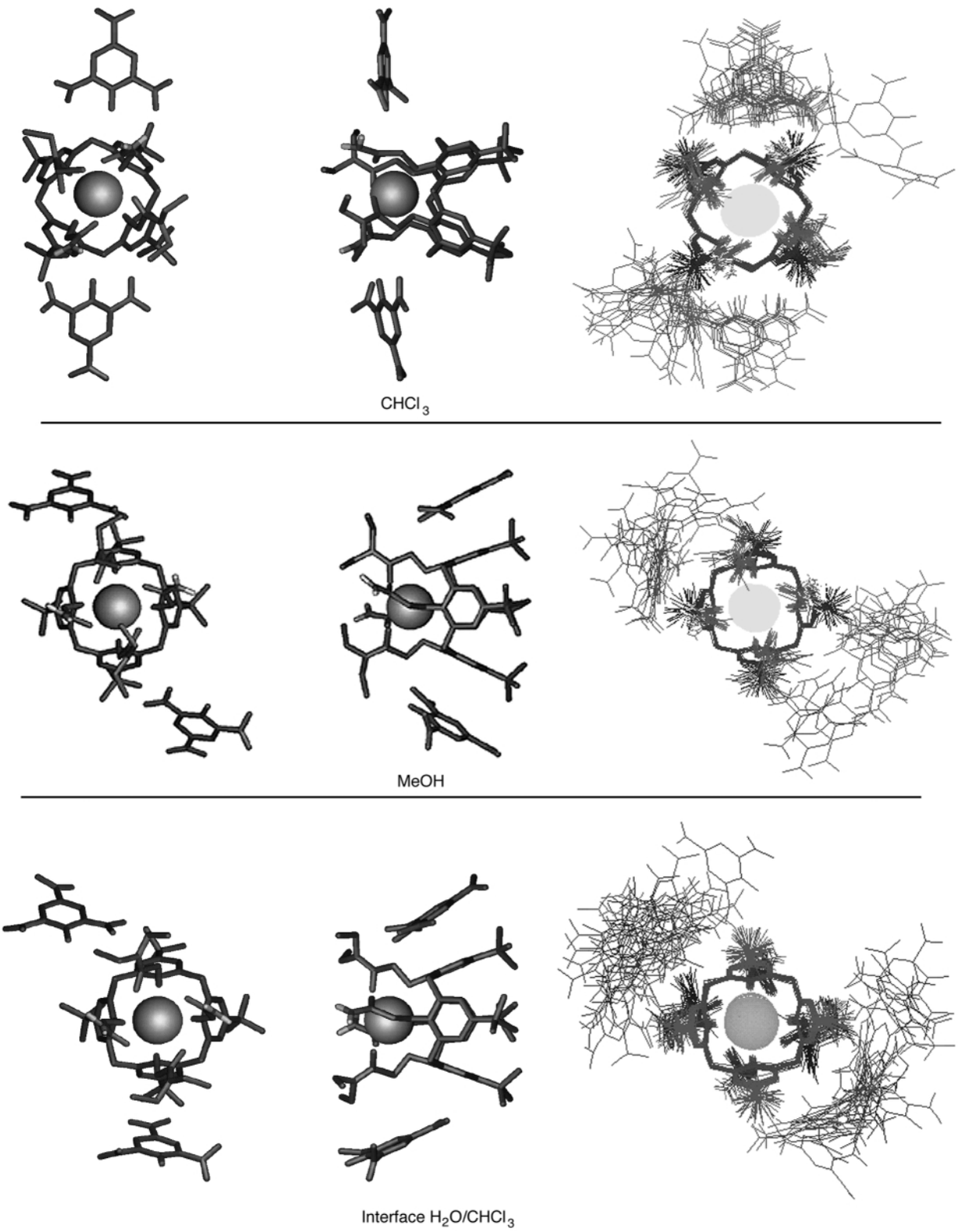

Fig. 5 The **L3**$SrPic_2$ complex simulated in chloroform, in methanol and at the water/chloroform interface. Left: snapshot at the end of the dynamics (orthogonal views); right: cumulated structures during the last 250 ps.

ion (−133 *versus* −72 ± 9 kcal mol^{-1}). A closer look reveals a different micro-environment for Sr^{2+} in the two cases. In the **L1** complex, it is completely shielded from water by the four amides. In the **L3** complex, the pseudo-cavity is unlocked by a water molecule directly coordinated to Sr^{2+}. As a result, the distance between opposite carbonyl oxygens is about 0.5 Å larger in the **L3** than in the **L1** complex (4.6 *versus* 4.1 Å, on average). Thus, *the increased attraction of the* **L3** *complex by water is not solely due to the hydrophobic/hydrophilic character of the N-ethyl/N–H groups, but also to subtle changes in the shape of the amidic pseudocavity which significantly modifies the interactions of the complexed cation with the solvent.* This analysis makes clear why the **L3** complex is more hydrophilic and surface active than the **L1** complex.

Discussion

The study of complexation and liquid–liquid extraction experiments by five different calix[4]arenes bearing various combinations of primary, secondary and tertiary amide sub-

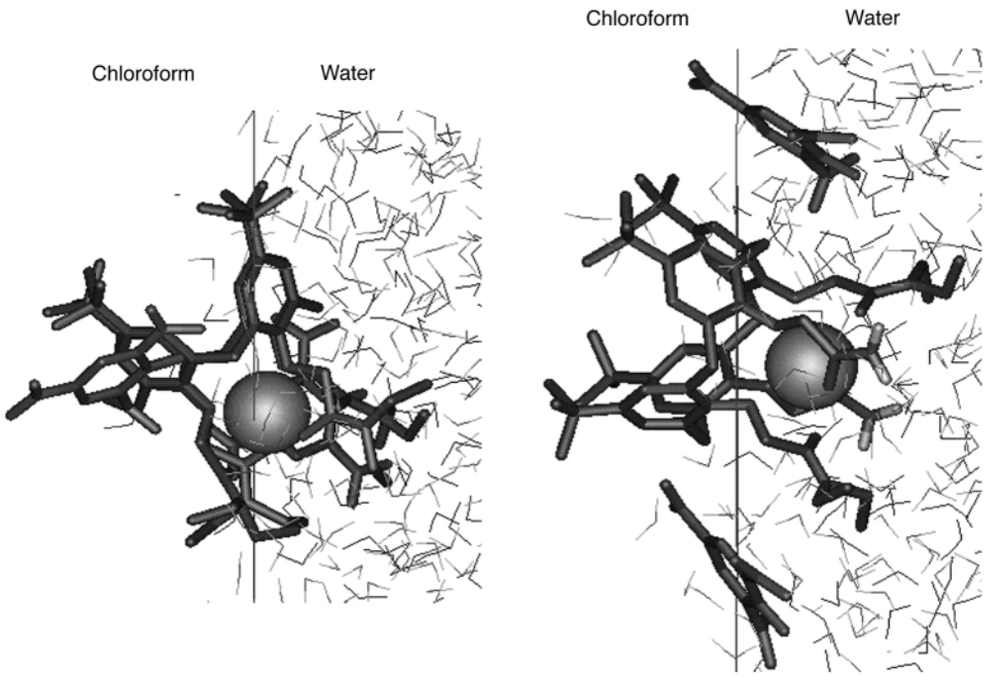

Fig. 6 **L1**Sr(Pic)$_2$ (left) and **L3**Sr(Pic)$_2$ (right) at the water/chloroform interface after 1 ns. Only selected water molecules are shown for clarity.

stituents highlights the following points. First, the cone conformation is important to allow for simultaneous interactions of the cation with the four amide arms. Second, there is an important effect of the substituents (alkyl/H) of the amide nitrogens on the binding strength in methanol as well as on the extraction capability of the ligands. In line with the reduced basicity of the amidic oxygen, the *N*-alkyl to *N*-H substitution weakens the interaction with the cation. This is supported by our QM calculations on small amide models in the gas phase, which show that the substituent effect is enhanced when the hardness of the cation increases, and in particular when trivalent lanthanides cations are bound by the amides. This feature is of general importance in related extractant molecules which incorporate amide binding sites.[34–36]

Less expected is the spectacular amide substituent effect on cation extraction from water to the organic phase. This may be due to a number of possible effects, relating to (i) the (unfavorable) conformation of the free ligand in the organic phase, (ii) the less effective ion–ligand interactions in the complexes, and (iii) interfacial phenomena. These different effects are discussed in the following.

The uncomplexed host may adopt in the organic phase a conformation unsuitable for cation binding. Based on NMR data alone, which reveal internal NH $\cdots$ O hydrogen bonds in **L3**, it could indeed be speculated that some energy cost has to be paid to change this conformer to the one with a pseudo-cavity suitable for cation complexation. However, according to the computer simulations, "negative preorganization" does not seem to be important: hydrogen bonding involves the O_{ether} more than the O_{amide} oxygens, and it does not correspond to a marked energy stabilization, relative to the other conformers in solution. In addition, the simulations do not reveal marked differences between NH $\cdots$ O_{ether} interactions in chloroform, compared to methanol solution. We also notice that in a water saturated organic phase, water-dragged molecules[37] may also bind to the NH groups, thus unlocking the calixarene ligands from unsuitable conformational states. Thus, internal hydrogen bonding in primary or secondary amide calixarenes does not seem to prevent the conformational changes of the ligands required for cation encapsulation.

A second possible explanation for the lack of ion extraction with primary or secondary amide derivatives concerns the effectiveness of cation–host interactions. According to our modeling studies on two typical systems, and by analogy with the complexation results in methanol, the nature of all the cone amide complexes should be similar, *i.e.* of 1 : 1 stoichiometry, with the cation similarly encapsulated in the pseudo-cavity delineated by the eight oxygen atoms of the host. Complexation data in methanol and modeling studies indicate that the cation becomes less firmly bound upon C(O)N–alkyl to C(O)N–H substitution. This effect alone is unlikely to prevent extraction by secondary or primary amides as they still complex the cations in methanol solution. In addition, one could anticipate that the NH groups of the secondary or primary amides facilitate the co-extraction of the accompanying anion *via* specific hydrogen bonding, as depicted in the simulations in pure chloroform solution. The reduced lipophilicity of these complexes compared to those with tertiary amides is another factor which acts against cation extraction.

The modelling studies at the interface point out an additional feature dealing with the mechanism of ion recognition. A number of theoretical studies[23,38,39] and of related experiments[40,41] demonstrate the high surface activity of substituted calixarene ligands, as well as of their cation complexes. From a mechanistic point of view, this implies that the cation capture takes place at the interface of the droplets formed upon shaking of the system.[23] As far as amide susbtituted ligands are concerned, it is clear that the *N*-alkyl to *N*-H substitution increases the surface activity and concentration of the free ligand at the interface. Based on the fact that such a substitution is not sufficient to prevent the cation complexation in methanol solution, we suggest that cation complexation by the calixarenes still likely occurs at the interface. However, the complexes with secondary or primary amide calixarene derivatives may be not lipophilic enough to diffuse into the organic phase. Modifying the lipophilic/hydrophilic balance of the ligand may also change the nature of the mixed phase, as do surfactants. Thus the nature of the mixed phases, as well as detailed events that take place at the interface are important questions which remain to be investigated by experiments as well as by computer simulations.

Acknowledgements

F. B. and N. M. thank the French Ministry of Research of a grant. A. C. and R. U. thank the MURST (Supramolecular

Devices Project) for financial support. This work is partly supported by the EU (F14WCT96 0022 project). G. W. thanks CNRS IDRIS and the University Louis Pasteur for computer resources.

References

1 G. D. Andreetti, F. Ugozzoli, A. Pochini and R. Ungaro, in *Inclusion Compounds*, ed. J. L. Atwood, J. E. D. Davies and D. D. MacNicol, Oxford University Press, Oxford, 1991, vol. 4, pp. 64–125; R. Ungaro and A. Pochini, in *Topics in Inclusion Science. Calixarenes, a Versatile Class of Macrocyclic Compounds*, ed. V. Böhmer and J. Vicens, Kluwer Academic Publishers, Dordrecht, 1990, pp. 127–145; M. J. Schwing and M. A. McKervey, *ibid.*, pp. 149–171; A. McKervey, M. J. Schwing-Weill and F. Arnaud-Neu, in *Comprehensive Supramolecular Chemistry*, ed. G. W. Gokel, Pergamon, Oxford, 1996, vol. 1, pp. 537–603.

2 S. Fanni, F. Arnaud-Neu, M. A. McKervey, M. J. Schwing-Weill and K. Ziat, *Tetrahedron Lett.*, 1996, **37**, 7975.

3 A. Arduini, E. Ghidini, A. Pochini, R. Ungaro, G. D. Andreetti, G. Calestani and F. Ugozzoli, *J. Inclusion Phenom.*, 1988, **6**, 119.

4 F. Arnaud-Neu, M. J. Schwing-Weill, K. Ziat, S. Cremin, S. J. Harris and M. A. McKervey, *New J. Chem.*, 1991, **15**, 33.

5 H. Sigel and R. B. Martin, *Chem. Rev.*, 1982, **82**, 385.

6 F. Arnaud-Neu, G. Barrett, S. Fanni, D. Marrs, W. McGregor, M. A. McKervey, M. J. Schwing-Weill, V. Vetrogon and S. Wechsler, *J. Chem. Soc.*, *Perkin Trans. 2*, 1995, 453.

7 S. K. Chang and I. Cho, *Chem. Lett.*, 1987, 947.

8 *Fourth European Conference on Management and Disposal of Radioactive Waste*, EUR 17543 EN, ed. T. McMenamin, European Communities Publications, 1997.

9 A. Casnati, Y. Ting, D. Berti, M. Fabbi, A. Pochini, R. Ungaro, D. Sciotto and G. G. Lombardo, *Tetrahedron*, 1993, **49**, 9815.

10 A. Casnati, C. Fischer, M. Guardigli, A. Isernia, I. Manet, N. Sabbatini and R. Ungaro, *J. Chem. Soc.*, *Perkin Trans. 2*, 1996, 395.

11 A. J. Speziale and P. C. Hamm, *J. Am. Chem. Soc.*, 1956, **78**, 2556.

12 H. A. Flashka, *EDTA Titration*, Pergamon Press, London, 1964.

13 A. Casnati, A. Pochini, R. Ungaro, F. Ugozzoli, F. Arnaud, S. Fanni, M. J. Schwing, R. J. M. Egberink, F. de Jong and D. N. Reinhoudt, *J. Am. Chem. Soc.*, 1995, **117**, 2767.

14 V. I. Vetrogon, N. G. Lukyanenko, M. J. Schwing-Weill and F. Arnaud-Neu, *Talanta*, 1994, **41**, 2105.

15 D. A. Pearlman, D. A. Case, J. C. Caldwell, W. S. Ross, T. E. Cheatham III, D. M. Ferguson, G. L. Seibel, U. C. Singh, P. Weiner and P. A. Kollman, *AMBER4.1*, University of California, San Francisco, CA, 1995.

16 P. A. Kollman, J. W. Caldwell, T. Fox, D. C. Spellmeyer, D. M. Ferguson, K. M. Merz, I. R. Gould, C. I. Bayly, P. Cieplak and W. D. Cornell, *J. Am. Chem. Phys.*, 1995, **117**, 5179.

17 N. Muzet, G. Wipff, A. Casnati, L. Domiano, R. Ungaro and F. Ugozzoli, *J. Chem. Soc.*, *Perkin Trans. 2*, 1996, 1065.

18 W. L. Jorgensen and J. Tirado-Rives, *J. Am. Chem. Soc.*, 1988, **110**, 1657.

19 G. Wipff and L. Troxler, *1st European Conference on Computational Chemistry*, 1995, pp. 325–336; L. Troxler, J. M. Harrowfield and G. Wipff, *J. Phys. Chem.*, 1998, **102**, 6821.

20 J. Aqvist, *J. Phys. Chem.*, 1990, **94**, 8021.

21 W. L. Jorgensen, J. Chandrasekhar and J. D. Madura, *J. Chem. Phys.*, 1983, **79**, 926.

22 W. L. Jorgensen, J. M. Briggs and M. L. Contreras, *J. Phys. Chem.*, 1990, **94**, 1683.

23 M. Lauterbach, E. Engler, N. Muzet, L. Troxler and G. Wipff, *J. Phys. Chem.*, 1998, **102**, 225; F. Berny, N. Muzet, R. Schurhammer, L. Troxler and G. Wipff, in *Current Challenges in Supramolecular Assemblies*, NATO ASI, ed. G. Tsoucaris, Kluwer Academic Publishers, Dordrecht, 1998, pp. 221–245 and references cited therein; F. Berny, N. Muzet, L. Troxler and G. Wipff, in *Supramolecular Science: where it is and where it is going*, NATO ASI, ed. R. Ungaro and E. Dalcanale, Kluwer Academic Publishers, Dordrecht, 1999, pp. 95–125; Lauterbach and G. Wipff, in *Physical Supramolecular Chemistry*, ed. L. Echegoyen and A. Kaifer, Kluwer Academic Publishers, Dordrecht, 1996, pp. 65–102; N. Muzet, E. Engler and G. Wipff, *J. Phys. Chem. B*, 1998, **102**, 10772; A. Varnek, L. Troxler and G. Wipff, *Chem. Eur. J.*, 1997, **3**, 552; L. Troxler and G. Wipff, *Anal. Sci.*, 1998, **14**, 43.

24 M. J. Frisch, G. W. Trucks, H. B. Schlegel, P. M. W. Gill, B. G. Johnson, M. A. Robb, J. R. Cheeseman, T. Keith, G. A. Petersson, J. A. Montgomery, K. Raghavachari, M. A. Al-Laham, V. G. Zakrzewski, J. V. Ortiz, J. B. Foresman, C. Y. Peng, P. Y. Ayala, W. Chen, M. W. Wong, J. L. Andres, E. S. Reploge, R. Gomperts, F. Martin, D. J. J. S. Binkley, D. J. Defrees, J. Baker, J. P. Stewart, M. Head-Gordon, C. Gonzales and J. A. Pople, Gaussian 94, Revision B.2, Gaussian, Inc., Pittsburgh PA, 1995.

25 P. Kaupp, P. v. R. Schleyer, H. Stoll and H. Preuss, *J. Chem. Phys.*, 1991, **94**, 1360.

26 M. Dolg, H. Stoll and H. Preuss, *J. Chem. Phys.*, 1989, **90**, 1730.

27 S. F. Boys and F. Bernardi, *Mol. Phys.*, 1970, **19**, 553.

28 L. C. Groenen, B. H. M. Ruël, A. Casnati, P. Timmerman, W. Verboom, S. Harkema, A. Pochini, R. Ungaro and D. N. Reinhoudt, *Tetrahedron Lett.*, 1991, **32**, 2675; A. Arduini and A. Casnati, *Calixarenes*, in *Macrocyclic Synthesis: a Practical Approach*, ed. D. Parker, Oxford University Press, Oxford, 1996, pp. 145–173.

29 C. D. Gutsche and L. J. Bauer, *J. Am. Chem. Soc.*, 1985, **107**, 6052; C. Jaime, J. de Mendoza, P. Prados, P. M. Nieto and C. Sanchez, *J. Org. Chem.*, 1991, **56**, 3372.

30 A. Casnati, A. Pochini, R. Ungaro, C. Bocchi, F. Ugozzoli, R. J. M. Egberink and D. N. Reinhoudt, *Chem. Eur. J.*, 1996, **2**, 436; I. Ikeda and S. Shinkai, *J. Am. Chem. Soc.*, 1994, **116**, 3102.

31 R. Taylor and O. Kennard, *Acc. Chem. Res.*, 1984, **17**, 320.

32 P. Murray-Rust and J. P. Glusker, *J. Am. Chem. Soc.*, 1984, **106**, 1018.

33 P. D. Beer, M. G. B. Drew, R. J. Knubley and M. I. Ogden, *J. Chem. Soc.*, *Dalton Trans.*, 1995, 3117.

34 G. Y. S. Chan, M. G. B. Drew, M. J. Hudson, P. B. Iveson, J.-O. Liljenzin, M. Skalberg, L. Spjuth and C. Madic, *J. Chem. Soc.*, *Dalton Trans.* , 1997, 649.

35 N. Condamines and C. Musikas, *Solv. Extract. Ion Exch.*, 1992, **10**, 69.

36 S. Musikas, P. Vitorge, R. Fitoussi, M. Bonin and D. P. Vialard-Goudou, International Symposium on Actinide Recovery, 182nd National Meeting of the American Chemical Society, 1981, pp. 1–14.

37 R.-S. Tsai, W. Fan, N. El Tayar, P. A. Carrupt, B. Testa and L. B. Kier, *J. Am. Chem. Soc.* , 1993, **115**, 9632.

38 G. Wipff and M. Lauterbach, *Supramol. Chem.*, 1995, **6**, 187.

39 G. Wipff, E. Engler, P. Guilbaud, M. Lauterbach, L. Troxler and A. Varnek, *New J. Chem.*, 1996, **20**, 403.

40 L. Dei, A. Casnati, P. L. Nostro, A. Pochini, R. Ungaro and P. Baglioni, *Langmuir*, 1996, **12**, 1589.

41 Y. Ishikawa, T. Kaïnite, T. Matsuda, T. Otsuka and S. Shinkai, *J. Chem. Soc.*, *Chem. Commun.*, 1989, 736.

Paper 9/02001B